

## Aerodynamic drag in competitive tandem para-cycling: Road race versus time-trial positions

Paul Mannion<sup>a,b,d,\*</sup>, Yasin Toparlar<sup>b</sup>, Bert Blocken<sup>b,c</sup>, Eoghan Clifford<sup>a,d</sup>, Thomas Andrianne<sup>e</sup>, Magdalena Hajdukiewicz<sup>a,d</sup>

<sup>a</sup> Department of Civil Engineering, National University of Ireland Galway, University Road, Galway, Ireland

<sup>b</sup> Department of the Built Environment, Eindhoven University of Technology, P.O. Box 513, 5600 MB, Eindhoven, the Netherlands

<sup>c</sup> Department of Civil Engineering, KU Leuven, Kasteelpark Arenberg 40 – Bus 2447, 3001, Leuven, Belgium

<sup>d</sup> Informatics Research Unit for Sustainable Engineering (IRUSE), Ireland

<sup>e</sup> Department of Aerospace and Mechanical Engineering, University of Liège, Allée de la Découverte, 9 Quartier Polytech 1, B52/3, B-4000, Liège, Belgium

### ARTICLE INFO

#### Keywords:

Tandem  
Paralympic  
Time-trial  
Para-cycling  
Aerodynamics  
Computational fluid dynamics  
Wind tunnel experiments

### ABSTRACT

An athlete's riding posture is a key element for aerodynamic drag in cycling. Tandem cycling has the complication of having two athletes in close proximity to each other on a single tandem bicycle. The complex flow-field between the pilot and stoker in tandem cycling presents new challenges for aerodynamic optimisation. Aerodynamic drag acting on two tandem road race setups and two track time-trial setups were analysed with computational fluid dynamics (CFD) simulations. For validation purposes, wind tunnel measurements were designed providing drag measurements from both tandem athletes simultaneously using a quarter-scale model. A max drag force deviation of 4.9% was found between the wind tunnel experiments and CFD simulations of the quarter-scale geometry. Full-scale CFD simulations of upright, crouched, time-trial and frame-clench tandem setups were performed. The drag force experienced by individual athletes in all investigated tandem setups was compared to that of solo riders to enhance understanding of the aerodynamic interaction between both tandem athletes. The most aerodynamic tandem setup was found to be the frame-clench setup which is unique to tandem cycling and had a  $C_D A$  of  $0.286 \text{ m}^2$ , and could provide an advantage of 8.1 s over a standard time-trial setup for a 10 km time-trial event.

### 1. Introduction

Tandem cycling is a sports branch governed by the International Cycling Union (UCI). Athletes who are visually impaired can compete in this discipline as the stoker, the rear athlete on the tandem bicycle. The lead athlete, denoted as the pilot, has full visual capabilities. The UCI has rules and restrictions over the suitability of an athlete to perform as a pilot, most notably, that members of a UCI professional team cannot perform as a tandem pilot, although it is allowed for former professional riders to do so (UCI, 2017).

Becoming faster by improving their aerodynamic profile is becoming a coveted prize for both elite and amateur cyclists. This is especially common within the core of elite cycling institutions across the world, both for able-bodied and para disciplines. Aerodynamic enhancements in elite able-bodied solo cycling have often traversed over to tandem cycling; in the form of aerodynamic wheel and frame designs, athlete

apparel, and athlete posture refinements. However, little is known about the fundamentals of tandem aerodynamics and how the air flow interacts with the pilot and the stoker. Thus, there are likely opportunities for aerodynamic refinements specific to tandem cycling with alternative posture combinations, athlete apparel, and equipment design. Typical tandem postures for individual tandem athletes are often similar to postures adopted by solo athletes (Fig. 1). These include upright, dropped, crouched and various time-trial (TT) postures. Postures can be athlete specific depending on the anthropometrics and flexibility of the riders. Postures can also exist specific to tandem cycling, such as the frame-clench stoker posture (Fig. 1b); used particularly in timed events. Here, the stoker grasps the top tube of the frame (just behind or under the pilot's saddle) instead of holding the handlebars in a track event, in an effort to 'hide' behind the pilot to a greater degree. The UCI has specific restrictions limiting the movement of the handlebars and the saddle, which are used for athlete posture adjustments. Additional rules limit the

\* Corresponding author. Department of Civil Engineering, National University of Ireland Galway, University Road, Galway, Ireland.

E-mail address: [p.mannion10@nuigalway.ie](mailto:p.mannion10@nuigalway.ie) (P. Mannion).

<https://doi.org/10.1016/j.jweia.2018.05.011>

Received 2 November 2017; Received in revised form 9 April 2018; Accepted 19 May 2018

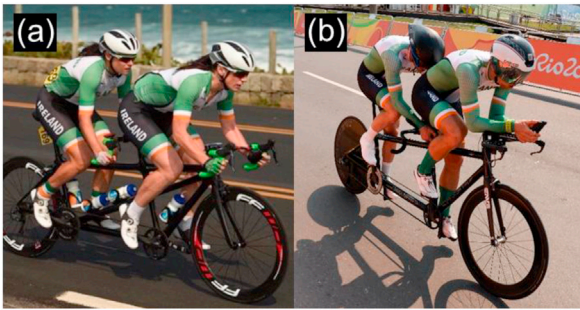


Fig. 1. (A) Irish female tandem team competing in a road race event, (b) Irish female tandem team competing in an outdoors TT event. The athletes in these photos were not involved in this research. © Sportfile, Cycling Ireland and Paralympics Ireland, reproduced with permission).

dimensions of the tandem frame tubes, and aerodynamic devices or attachments are not permitted (UCI, 2017). These rules apply to both tandem and solo competitive cyclists, and are intended to keep the competition both fair and safe for all athletes participating.

CFD simulations and wind tunnel testing have been widely used in sports engineering in general and in cycling aerodynamics studies in particular (Blocken, 2014; Crouch et al., 2017). To the best of our knowledge, only Mannion et al. (2017) published a CFD and wind tunnel investigation on tandem cycling aerodynamics. Mannion et al. (2017) presented new guidelines for the modelling of tandem aerodynamics using CFD, and determined that the accurate prediction of flow separation is crucial for the appropriate assessment of tandem aerodynamics using CFD. Hence, a low average  $y^*$  value less than 1 was recommended when generating a grid for a tandem cycling case study. Counter-intuitive and incorrect drag occurrences between the pilot and the stoker were observed when this guideline was not followed, with the stoker experiencing a larger drag force than the pilot. Mannion et al. (2017) also highlighted the impact of selecting a suitable turbulence model for tandem cycling aerodynamics, with the SST  $k-\omega$  model (Menter, 1994) recommended for tandem cycling aerodynamics research. This is in agreement with the findings of Defraeye et al. (2010b) who also determined that the SST  $k-\omega$  turbulence model provided the best overall predictions for solo cyclist aerodynamics, through obtaining detailed validation data from wind tunnel experiments with pressure measurements in addition to force and moment measurements.

Within the remaining literature, tandem cycling bears a close resemblance to a two-rider drafting formation; where two athletes cycle in close proximity and in-line with each other in order to provide a drag reduction primarily for the trailing cyclist. However, Blocken et al. (2013) determined through CFD simulations that the leading cyclist in a two-rider drafting formation can experience a reduction in drag by up to 2.6%. The benefit that a leading cyclist can gain was found to be enhanced if, instead of a trailing cyclist, a motorbike or a car was behind the cyclist (Blocken and Toparlar, 2015; Blocken et al., 2016). Indeed, a cyclist was found to experience drag reductions of up to 8.7% from a single following motorbike. The flow structures around two reduced scale in-line cyclists were analysed experimentally by Barry et al. (2016), who observed that the wake flow of the trailing cyclist was characteristic of that from a solo cyclist. Full scale wind tunnel experiments on two drafting cyclists were conducted by Barry et al. (2014), who found that the leading and trailing cyclists experienced maximum drag reductions up to 5% and 49% respectively.

Competitive solo cyclist postures and cycling positions have been widely researched in the literature, for both optimal power output and aerodynamics (Gnehm et al., 1997; Oggiano et al., 2008; Defraeye et al., 2010a; Underwood and Jermy, 2010; Chabroux et al., 2012; Fintelman et al., 2014a, 2015) where both computational and experimental methods have been successfully utilised to determine optimal postures for athletes. Defraeye et al. (2010a) conducted CFD analyses of solo

cycling postures; upright, dropped and TT, and results from full-scale wind tunnel experiments were used to validate the computational results;  $C_D A$  values of  $0.270 \text{ m}^2$ ,  $0.243 \text{ m}^2$  and  $0.211 \text{ m}^2$  were obtained for the upright, dropped and TT postures respectively from the wind tunnel experiments. Fintelman et al. (2014a) concluded that athletes should balance power output with aerodynamics, but determined that aerodynamic losses exceeded physical power losses at a velocity of 46 km/h, indicating that the importance of aerodynamics may outweigh the importance of power delivery at high speeds. Barry et al. (2015b) conducted wind tunnel experiments using solo cyclists to determine the influence of various athlete postures on aerodynamic drag. It was found that an optimal aerodynamic solution was for the athlete to bring his arms inside the silhouette of his torso and hips. It was also found that for an athlete in a dropped posture for a road race setup, the power requirement to maintain the same velocity can drop by 7% by lowering the head and torso to a crouched posture with horizontal forearms.

To the best knowledge of the authors, there has been no research on tandem posture variations conducted in the literature, and with no appearance in relevant review papers (Crouch et al., 2017; Lukes et al., 2005). Given the number of aerodynamic posture refinements that are applicable for a solo cyclist, there is an extensive scope of research for tandem athletes yet to be conducted. Readers are referred to Defraeye et al. (2010a) for a comparative summary of drag data for various solo cycling postures in the early cycling aerodynamics literature (1980's – 2000's).

The research presented here addresses the predominant gap in the literature regarding typical tandem athlete posture combinations. CFD simulations are performed by solving the 3D Reynolds-averaged Navier-Stokes (RANS) equations to explore the aerodynamics of two typical tandem road setups, and two tandem track TT setups. Fig. 1 shows two examples of competitive tandem cyclists with athlete posture combinations for a road race and outdoor TT event. Wind tunnel experiments are used to provide validation data for the CFD simulations.

## 2. Wind tunnel experiments

Wind tunnel experiments were devised to provide drag data on both the pilot and the stoker individually. Wind tunnel experiments were carried out in the aeronautical test section of the wind tunnel laboratory in the University of Liège, Belgium. A single athlete was 3D scanned using an Eva structured light scanner (Artec Europe, 2017) in a crouched posture, relevant to both pilot and stoker positions. By using the same geometrical athlete model for both the pilot and stoker positions, any inferred drag bias raised due to anthropometrical differences between two different athletes was removed. Quarter-scale 3D models were manufactured for the pilot, stoker and tandem bicycle by CSC cutting (Fig. 2). Similar to the set-up in Blocken et al. (2016), the model was raised 0.3 m from the bed of the test section by a sharp edged horizontal platform to limit the boundary layer development upstream of the test geometries. The resulting blockage in the  $2 \text{ m} \times 1.5 \text{ m}$  test chamber with

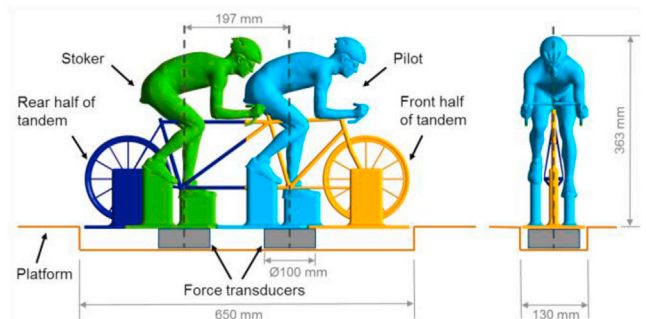


Fig. 2. Quarter-scale tandem geometry used for the wind tunnel experiments with the two force transducers.



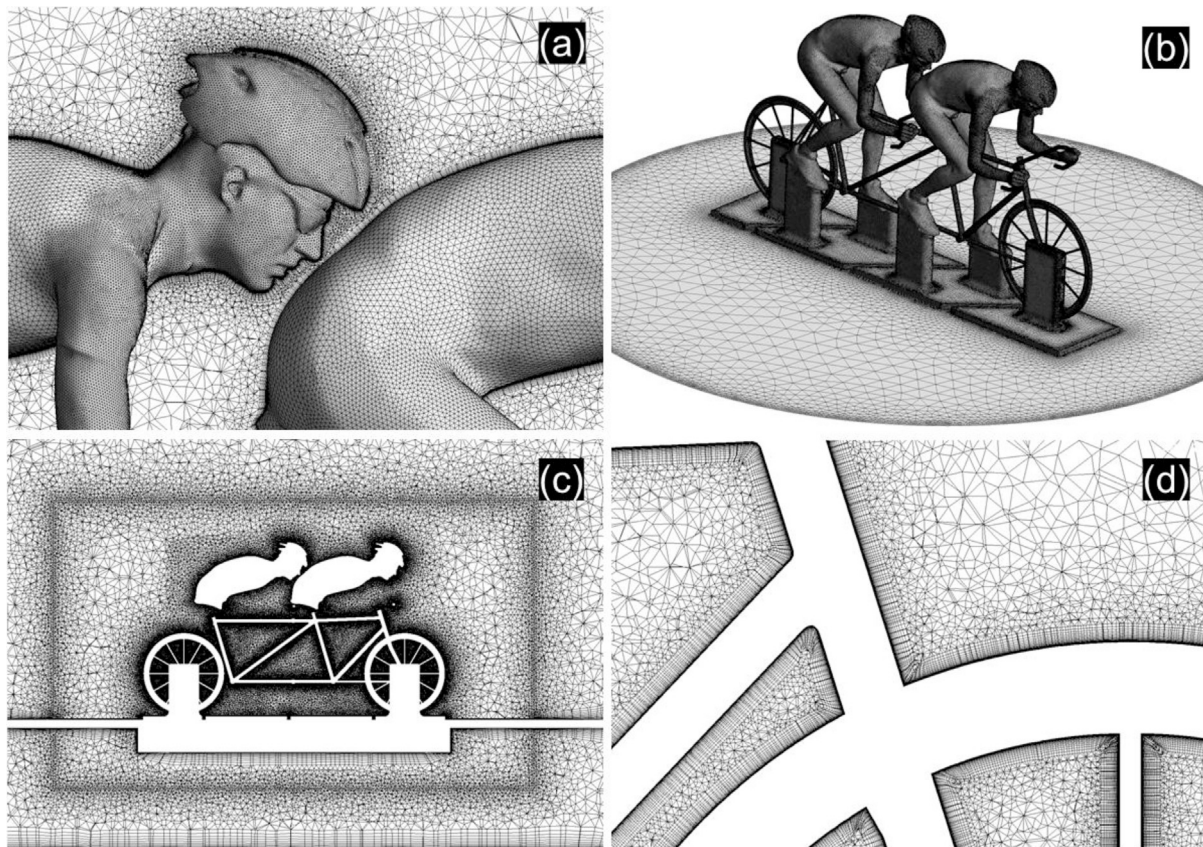


Fig. 4. (A) Part of the surface grid on the tandem athletes, (b) part of the surface grid on the platform and tandem geometry (c) part of the volume grid in a vertical plane for the tandem geometry in the modelled wind tunnel environment (d) part of the volume grid around the front wheel rim, spokes, and front frame tube members (number of cells: 46,167,727).

### 3.4. Comparison of results with wind tunnel experiments

As shown in the colour coded Fig. 2, the drag measurements for both the pilot and the stoker included their respective handlebars and foot supports. The drag experienced by the bicycle was not recorded in the wind tunnel experiment, and hence is not discussed for the validation of the CFD simulations. The resulting drag forces on the pilot and the stoker at both yaw angles tested are displayed in Fig. 5, for both the wind tunnel experiments and CFD simulations. The drag predictions were representative of the x-axis of the force transducers which were yawed along with

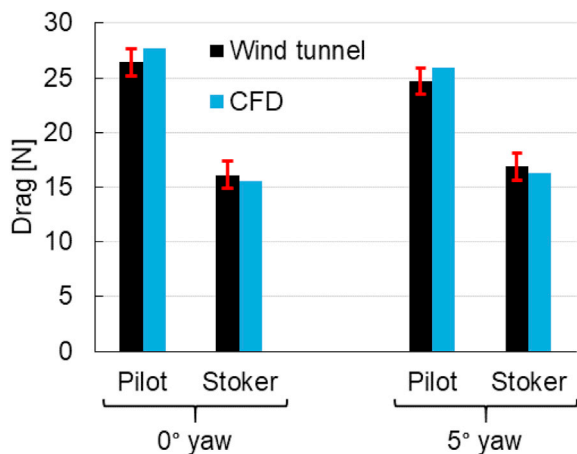


Fig. 5. Comparison of drag forces from wind tunnel experiments and CFD simulations at yaw angles of 0° and 5°. The error lines denote the margin of errors due to the measurement equipment.

the tandem model, and not held in the stream-wise flow direction. Thus, the transducers x-axis remained aligned with the tandem geometry. At 0° yaw, the CFD simulations drag predictions deviated by 4.7% for the pilot, and by -3.4% for the stoker. At 5° yaw, further good agreement between the CFD and wind tunnel experiments was observed for the pilot with a deviation of 4.9%. The CFD drag prediction for the stoker at 5° yaw deviated again by -3.4% from the wind tunnel result. The absolute difference between the CFD and wind tunnel experiments for all drag measurements was within the 1.24 N error range of the force transducers used in the experiments.

Good agreement and consistency was found between the wind tunnel experiments and CFD simulations (<5% drag deviation). Thus, the settings and parameters used for the CFD simulations were considered suitable for the analysis of variations of the tandem geometry, i.e. road and TT event setups. The same athlete and the same basic bicycle geometry were used for all further studies, with the position of the legs identical for all posture variations investigated.

## 4. Comparison of tandem setup variations

### 4.1. Geometrical models

Four tandem geometries were developed for aerodynamic analysis using CFD as shown in Fig. 6; upright, crouched, time-trial (TT) and frame-clench (FC). Due to varying athlete anthropometrics, there is a wide variety of possible tandem athlete positions, some unique to the individual pairs of athletes. Thus, this study uses the same rider for both pilot and stoker positions to provide non-biased results. The upright setup is not commonly adopted in competitive cycling events and it is most commonly used for casual non-competitive tandem cycling, or for

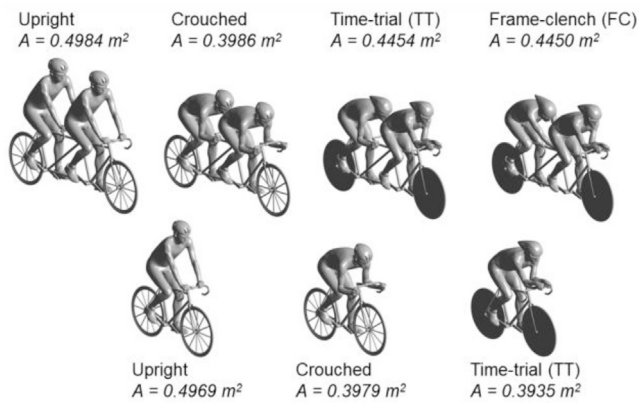


Fig. 6. Tandem and solo setups with frontal area comparisons.

warming up or relaxing at the beginning or the end of a competitive event. However, it provides an interesting comparison to other tandem postures. In this setup, both athletes wore a road helmet and spoked wheels were fitted to the bicycle geometry. The athletes had their hands on the upper part of a standard handlebar with outstretched arms. The crouched setup featured both the pilot and stoker in an aggressive drops posture with bent elbows, forearms parallel to the road, wearing road helmets, and with spoked wheels fitted to the bicycle geometry. The stoker in the TT setup adopted a crouched posture, wearing a TT helmet. The pilot in the TT and FC setups adopted a typical solo TT posture with their arms resting on elbow pads. The stoker in the FC setup (used in time-trial events), exhibited a torso angle similar to that of the crouched posture, but did not use the handlebars. Instead, the stoker grasped the top tube of the tandem bicycle in the vicinity underneath the pilot's saddle. The exact location of grasping the frame can vary depending on individual rider preferences. For this study, the stoker grasped the intersection of the top tube and seat tube below the pilot's saddle. The stoker's head was tilted towards the ground to a larger degree than that of the crouched posture, which can be typical of a stoker athlete when grasping the frame over the handlebars (Fig. 1b). Both the TT and FC setups were representative of track TT events, with two disk wheels fitted to the bicycle, while the riders wore teardrop shaped TT helmets. The location of the legs within the 360° crank cycle in each tandem setup was identical. During scanning of the actual athlete body, a wooden pedal stopper was used to ensure uniformity in the location of the legs between 3D scans of different postures, where the left crank (athlete perspective) was positioned at an angle of 20° anticlockwise to the horizontal plane.

Three solo geometries were created, representative of an upright, crouched and TT setup (Fig. 6). These solo geometries used the same athlete's geometrical model as their respective tandem counterparts. By modelling these athlete postures in a solo scenario, it was possible to gain further understanding on the flow interaction between the pilot and stoker, determining the effect each athlete has on the flow-field around the other. The same grid parameters for the tandem geometries were applied to the solo geometry for equivalent geometrical features, using the sizings discussed in section 3.2 scaled to the full-scale geometry.

For both tandem and solo setups, the bicycle geometry was simplified to keep the computational grid from exceeding the capability of the available computational resources. Items such as the chain and sprocket, derailleurs, brake mechanisms and handles were neglected. The spoked wheels were also simplified as per the 3D model for the wind tunnel experiment; twelve spokes with diameters of 0.012 m. Some geometric detail was added, in comparison to the validated case study (section 3), including frame forks, cranks, pedals, and frame members that previously, in the experimental setup, were removed or simplified. Each tandem setup was raised 0.02 m from the ground surface to prevent skewed cells forming at the location where the ground surface would be tangent to the wheels. All wheels and athletes' geometries were considered as static within the simulations.

## 4.2. Simulation settings and parameters

The computational domain used for the full-scale tandem and solo cyclists was described by an  $80 \times 28 \times 28 \text{ m}^3$  cuboid, which kept the maximum blockage ratio below the recommended by Blocken (2015), Franke et al. (2007), and Tominaga et al. (2008). The tandem geometry was located 28 m from the inlet boundary condition and centred laterally in the domain. The surfaces of the athletes and bicycle geometries were modelled using a no-slip wall with zero roughness. A uniform velocity of 15 m/s with a 0.2% turbulence intensity was used for the inlet condition, and a 0 Pa static gauge pressure was imposed for the outlet condition. A symmetry condition with zero-normal gradients was applied to the side surfaces of the domain. A pseudo time-step size of 0.01 s was used for these full-scale simulations. The grids for the full-scale tandem geometries were scaled up from the quarter-scale simulations discussed in section 3.2. The solo cyclist geometries received identical grid sizing as the tandem simulations on respective athlete and bicycle surfaces to ensure good comparability. Grid sizes are provided in Fig. 7. All other numerical simulations in this section utilised the same CFD solver parameters as outlined in section 3.3.

Target parameters included the drag area [ $\text{m}^2$ ] and pressure coefficient [–]. The drag area is given by:

$$C_{DA} = \frac{F_D}{0.5\rho V^2} \quad (1)$$

where  $F_D$  is the drag force [N],  $A$  is the frontal area [ $\text{m}^2$ ],  $\rho$  is the density [ $\text{kg}/\text{m}^3$ ], and  $V$  is the free-stream velocity [m/s]. The pressure coefficient is defined as:

$$C_P = \frac{\Delta P}{0.5\rho V^2} \quad (2)$$

where  $\Delta P$  [Pa] is the pressure difference between the location of interest and the reference pressure.

## 4.3. Aerodynamic analysis of different setups

The CFD simulations for the different tandem setups showed that the upright setup produced the highest  $C_{DA}$  of  $0.413 \text{ m}^2$ , while the crouched tandem setup produced a lower  $C_{DA}$  of  $0.314 \text{ m}^2$ . The TT and FC tandem setups yielded similar aerodynamic performance to each other with only 2.4% difference between their  $C_{DA}$  predictions. The FC setup was the more aerodynamic of the two with a  $C_{DA}$  of  $0.286 \text{ m}^2$ , against  $0.293 \text{ m}^2$  predicted for the TT setup. The solo cyclists experienced  $C_{DA}$  values of  $0.327 \text{ m}^2$ ,  $0.233 \text{ m}^2$  and  $0.213 \text{ m}^2$  for the upright, crouched and TT setups respectively. Fig. 7 compares  $A$ ,  $C_D$ , and  $C_{DA}$  values.

The drag experienced by the tandem athletes for each posture combination, and for the solo geometries is plotted in Fig. 8 without the bicycles included in the drag summations. The pilot and stoker contributed 54.7% and 29.2% respectively to the total drag when adopting upright postures. Respective contributions were 52.4% and 27.0% when crouched postures were adopted. A comparison of the drag interaction between the pilot and stoker for the TT and FC setups presented interesting results relevant to attaining optimisations for tandem athletes. The TT posture the pilot adopted was identical for both the TT and FC tandem setups. For the FC setup, the stoker clenched the frame rather than the handlebars, and tilted his head slightly towards the ground. The stoker in the standard TT setup adopted a crouched posture identical to that of the crouched setup, and experienced 3.8% more drag than the stoker of the FC setup as a result. The pilot of the FC setup also benefited from the posture adopted by the stoker, and experienced 5.1% less drag than the pilot in the standard TT setup, despite the geometrical models of both the TT and FC pilots being the same. This indicates that adjusting the stoker's posture not only provided less drag to the stoker, but also helped to reduce the drag of the pilot. The percentage contributions of the TT and

		No. cells	A [m <sup>2</sup> ]	C <sub>D</sub> [-]	C <sub>D</sub> A [m <sup>2</sup> ]	C <sub>D</sub> A [m <sup>2</sup> ]				
						0.0	0.1	0.2	0.3	0.4
Tandem	Upright	36209228	0.4984	0.829	0.413	[Bar chart showing C <sub>D</sub> A value of 0.413]				
	Crouched	40449677	0.3986	0.788	0.314	[Bar chart showing C <sub>D</sub> A value of 0.314]				
	TT	29589253	0.4454	0.658	0.293	[Bar chart showing C <sub>D</sub> A value of 0.293]				
	FC	30833092	0.4450	0.643	0.286	[Bar chart showing C <sub>D</sub> A value of 0.286]				
Solo	Upright	26523083	0.4969	0.658	0.327	[Bar chart showing C <sub>D</sub> A value of 0.327]				
	Crouched	29176392	0.3979	0.586	0.233	[Bar chart showing C <sub>D</sub> A value of 0.233]				
	TT	17817311	0.3935	0.541	0.213	[Bar chart showing C <sub>D</sub> A value of 0.213]				

Fig. 7. Comparison of C<sub>D</sub> [-] and C<sub>D</sub>A [m<sup>2</sup>] values as predicted by the CFD simulations for the tandem and solo geometries, with the number of cells per simulation and the projected frontal areas [m<sup>2</sup>].

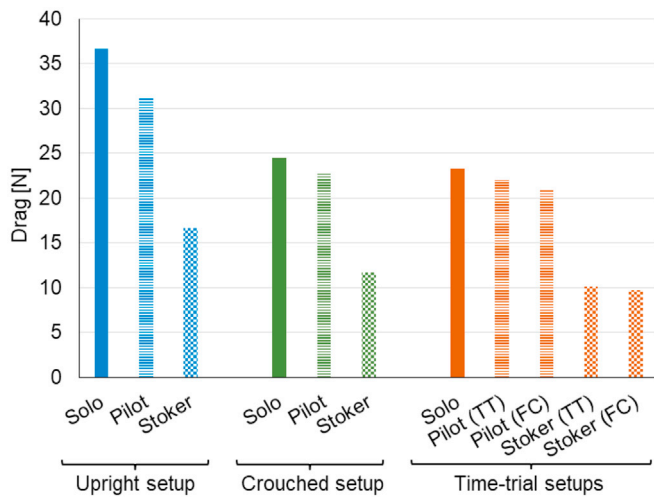


Fig. 8. Comparison of drag forces experienced by the athletes with different postures for solo and tandem setups.

FC athletes to their total drag was similar to the crouched setup, with contributions of 54.6% and 25.1%, and 53.3% and 24.7% for the pilots and stokers respectively. By comparison, the solo TT athlete contributed to 79.2% of their total drag with the bicycle experiencing the remaining 20.8%. Note that despite the differences in bicycle geometry, the sum of the drag contributions of the TT and FC athletes is the equivalent sum of the solo athlete drag contribution ( $\approx 79\%$ ).

Both athletes on all tandem setups received an aerodynamic benefit from the other athlete, pilot or stoker. In the following, a comparison is provided of the drag of the isolated tandem athletes relative to the drag experienced by a solo rider in an equivalent posture. The upright and crouched setup geometries had identical athlete geometry for their respective tandem and solo athletes. Thus, reasonable comparisons can be made between the athletes with the drag isolated from the bicycles. Compared to their solo cyclist equivalent, the upright tandem pilot experienced a drag reduction of 15.1% by the presence of the stoker, who experienced a drag reduction of 54.6% by the presence of the pilot. The drag reductions for the crouched and TT pilots and stokers by comparison to their solo cyclist counterparts were 7.3% and 52.2%, and 5.4% and 56.6% respectively. The FC tandem setup was the most aerodynamically efficient tandem setup. By comparison to the TT solo cyclist, the pilot saved 9.9% in drag force due to the presence of the stoker, and the stoker in the FC setup experienced a 58.2% reduction in drag. The arms of the stoker in the FC setup were in close proximity to the pilot, which assisted in the drag reduction of both the pilot and the stoker by reducing the under-pressure on the back of the pilot and the over-pressure on the arms

of the stoker. It is noted that this is a generalised comparison for the TT setups; the solo TT athlete and tandem TT and FC stokers do not share identical geometries, where the stoker athletes grasp the handlebars and frame respectively. In addition, there are differences between the tandem and solo bicycle geometry (additional frame tubes, handlebars etc.) whose interference flow affects all solo and tandem athlete comparisons. However, the comparisons to the solo riders remain useful to generate further understanding of tandem aerodynamics.

Pressure coefficient contours on the surfaces of the two road and two TT setups in tandem cycling are plotted in Figs. 9 and 10 respectively. Pressure coefficient contours for the three comparison solo geometries are also plotted in Figs. 9 and 10 alongside the tandem geometries for comparison purposes. These contours provide insights into the flow interaction between the pilot and stoker. The difference in pressure coefficient on the torsos of both the pilot and stoker is apparent for all posture combinations (Fig. 9–10). In comparison to equivalent solo athletes, all stoker athletes experienced a reduced maximum pressure on their frontal areas due to the presence of the pilot, while the pressure distribution on the front of the tandem pilots was comparable to that of the solo equivalent solo athlete.

The pressure coefficient contours for the solo setups (Fig. 9–10) highlight the importance of the flow interaction between the pilots and stokers. The subsonic upstream pressure (Blocken et al., 2013) imparted from the stoker in all tandem setups decreased the absolute value of the pressure coefficient on the back of the pilot, and reduced the severity of the pressure gradient on the outer sides of the pilot's torso and legs (by comparison to equivalent solo athletes). A general comparison of all pilots to their stokers revealed notable differences in pressure gradients from the upper arms, on the side of the torsos, and on the legs. While the pressure gradients were located at similar positions on the stoker as the pilot, the pressure gradients were not as large over the stoker as they were over the pilot.

## 5. Discussion

### 5.1. Evaluation of the numerical findings

The tandem FC setup proved to be the most aerodynamic setup analysed with a C<sub>D</sub>A of 0.286 m<sup>2</sup>, and experienced air resistance 2.4% lower than the standard TT tandem setup. The tandem crouched setup produced a C<sub>D</sub>A of 0.314 m<sup>2</sup>, 7.2% larger than the tandem TT setup, which experienced a C<sub>D</sub>A of 0.293 m<sup>2</sup>. The solo crouched setup was found to experience 9.4% more drag than the solo TT setup, with C<sub>D</sub>A values of 0.233 m<sup>2</sup> and 0.213 m<sup>2</sup> respectively. The low torso angle and horizontal forearms of the crouched postures contributed to their good aerodynamic performance by comparison to the TT postures, with drag differences less than 10% found for both the tandem and solo setups between their respective crouched and TT setups. The upright tandem setup experienced

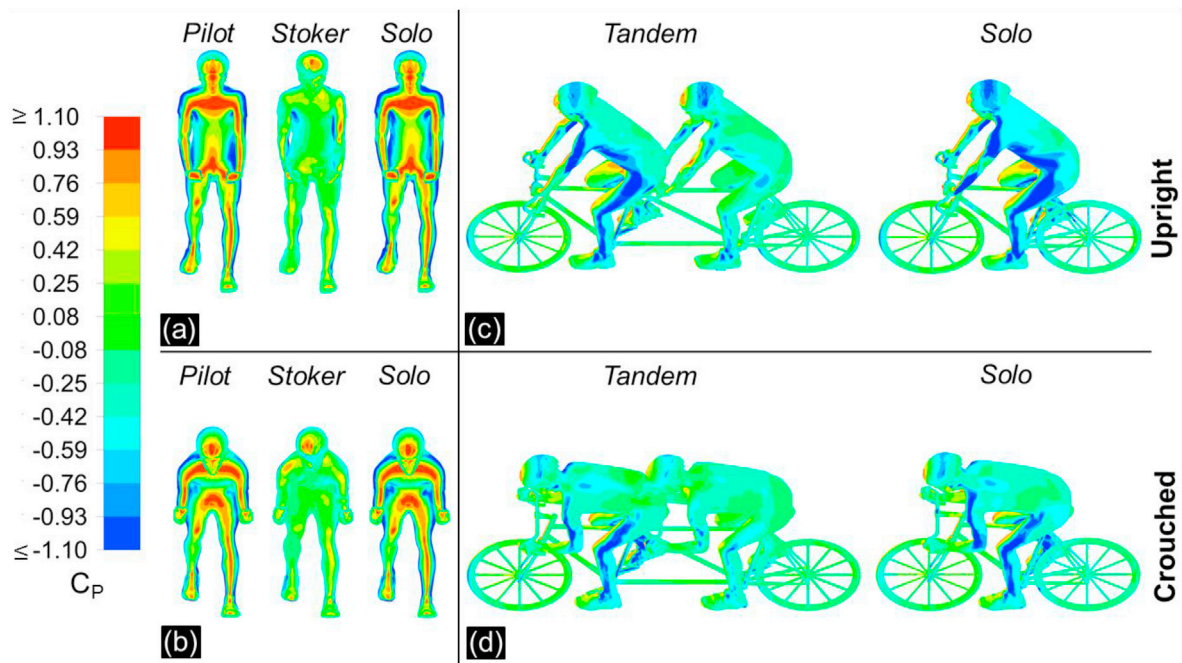


Fig. 9. Pressure coefficient contours on the projected frontal areas of the pilot, stoker and solo athletes for (a) an upright setup, and (b) a crouched setup. Pressure coefficient contours are presented on a complete tandem and solo geometries for a (c) upright, and (d) crouched setups.

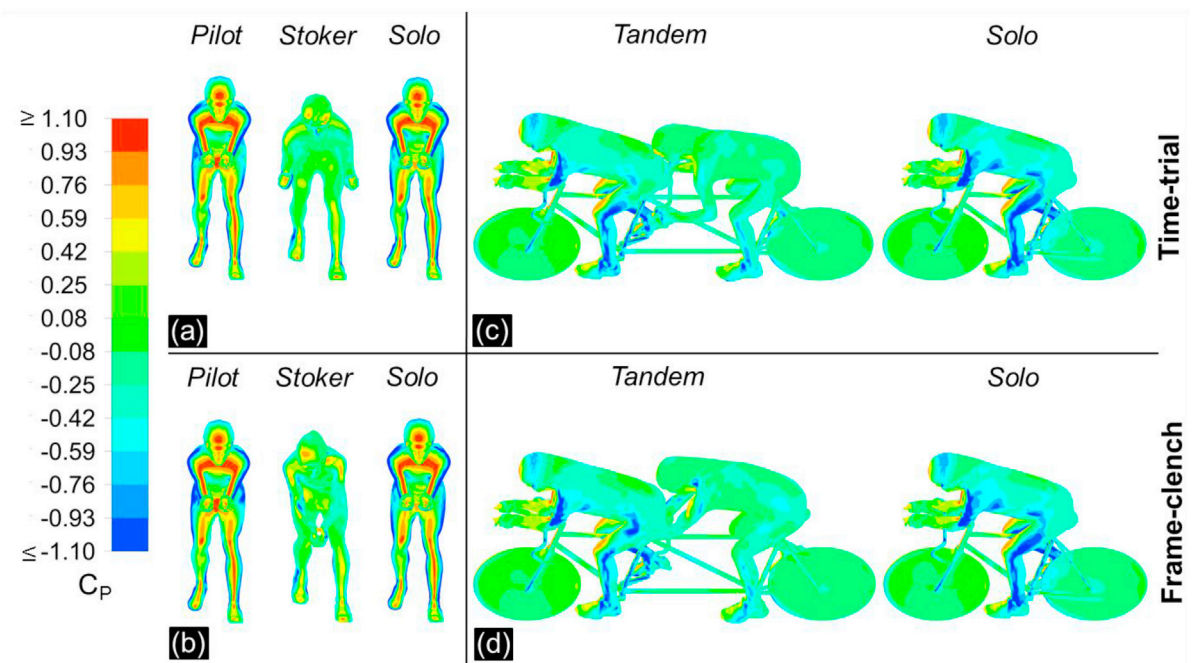


Fig. 10. Pressure coefficient contours on the projected frontal areas of the pilot, stoker and solo athletes for (a) a time-trial setup, and (b) a frame-clench setup. Pressure coefficient contours are presented on the complete tandem and solo geometries for a (c) time-trial, and (d) frame-clench setups.

31.3% more drag than the crouched tandem setup for comparison. The difference in aerodynamics between the tandem setups can be converted into time differences over a racing distance of 10 km, assuming that all tandem setups deliver a power output equal to that required for the FC setup to travel at 15 m/s. In this scenario the crouched tandem setup would travel 1.83 m/s faster than the upright setup and would theoretically finish the 10 km race 102.6 s earlier. Under the same conditions, the FC tandem would finish 8.1 s before the TT tandem, travelling 0.18 m/s faster. It is also interesting to compare a tandem and solo

setup, albeit under idealised conditions and considering aerodynamic variables only. If we consider the crouched solo rider, and the two tandem athletes in crouched postures from this study, and further consider that each athlete outputs the same power of 300 W; the tandem would have a velocity 14.1% higher than the solo bicycle, completing a distance of 10 km 96.3 s before the solo rider. Furthermore, if the tandem travelled at the same velocity as the solo rider, each tandem athlete would consume only 67.4% of the energy that the solo rider expends to overcome aerodynamics.

**Table 1**

CDA values from the literature, where full-scale wind tunnel experiments were conducted on static solo cyclists and their bicycles, whose postures were a close match to those used in the present research with photographic or descriptive evidence. BR = blockage ratio. TI = turbulence intensity. Open/Closed refers to the test section type of the wind tunnel.

Author	C <sub>D</sub> A [m <sup>2</sup> ]			Wind tunnel operating parameters		
	Upright	Crouched	Time-trial	Open/Closed	BR (%)	TI (%)
Fintelman et al. (2014b)	0.330 <sup>a,g</sup>			Open	12.5 <sup>i</sup>	0.67
Defraeye et al. (2010a)	0.270 <sup>b</sup>			Closed	6	0.02
Fintelman et al. (2014b)		0.300 <sup>c,g</sup>		Open	12.5 <sup>i</sup>	0.67
Kyle and Burke (1984)		0.249 <sup>d</sup>		Closed	6 <sup>i</sup>	–
Griffith et al. (2014)			0.201 <sup>e</sup>	Open	4	1.6
Defraeye et al. (2010a)			0.211	Closed	5	0.02
García-López et al. (2008)			0.260 <sup>f</sup>	Closed	6 <sup>i</sup>	–
Present research (numerical)	0.327	0.233	0.213	–	0.06 <sup>k</sup>	0.2 <sup>k</sup>

<sup>a</sup> From Fig. 4 Fintelman et al. (2014b).

<sup>b</sup> Disk wheels and a time-trial helmet were used in contrast to spoked wheels and a standard road helmet in the present research.

<sup>c</sup> Dropped posture with torso angle of 16°, not as aggressive as a crouched posture but a useful comparison.

<sup>d</sup> From Fig. 1 by Kyle and Burke (1984).

<sup>e</sup> From Fig. 3 by Griffith et al. (2014) at a crank angle of 15°, similar to the angle adopted in the present research.

<sup>f</sup> Spoked wheels were used in contrast to disk wheels used in the present research.

<sup>g</sup> Blockage corrections by Mercker & Wiedemann (1996) applied.

<sup>i</sup> Assuming a frontal area of 0.4 m<sup>2</sup>.

<sup>j</sup> Assuming a frontal area of 0.5 m<sup>2</sup>.

<sup>k</sup> Values from CFD boundary conditions.

## 5.2. Comparison with prior research

### 5.2.1. Tandem cycling

Since prior studies on tandem cycling are limited, a useful comparison of percentage drag reductions can be made to the published material on drafting in the literature. In a drafting scenario, a cyclist takes advantage of energy saved by being in the wake of an upstream cyclist. The work by Blocken et al. (2013) holds many comparable aspects to the present research. It was found that the over-pressure at the front and the under-pressure on the back of the trailing cyclist were reduced by the presence of the leading cyclist, who in turn received a benefit from the over-pressure in front of the trailing cyclist. Static CFD simulations were considered for the two inline cyclist geometries. The bicycle was neglected from the cyclist geometries; however, this allows for more direct comparison to the drag experienced by the athletes in the present research when isolated from the tandem bicycle. Upright, dropped and TT athlete postures were tested. The maximum benefit found for the lead rider of a two-formation drafting scenario was 2.6%. The benefit was acquired from the presence of the trailing rider, who experienced a maximum drag reduction of 27.1%. These maximum benefits were measured for a minimum wheel to wheel distance of 0.01 m. The percentage benefit to both the leading and trailing riders were found to be dependent on the posture adopted by the athlete, and the spacing between them. The maximum drag saving recorded in the tandem studies in the present paper was 15.1% and 58.2% for the pilot and stoker of the upright and FC setups respectively. These findings were in excess of the maximum savings recorded by Blocken et al. (2013) as expected due to the closer proximity of the tandem athletes on the tandem bicycle. Barry et al. (2014) conducted wind tunnel experiments of two full-scale drafting cyclists, and confirmed the earlier findings by Blocken et al. (2013) that the leading cyclist in a drafting formation benefitted aerodynamically from the trailing cyclist. At the minimum inline wheel to wheel separation distance ( $\approx 0$  m), drag reductions of 5% and 49% were recorded for the leading and trailing cyclists (athlete and bicycle) respectively.

### 5.2.2. Solo cycling

The solo upright, crouched and TT postures produced C<sub>D</sub>A values of 0.327 m<sup>2</sup>, 0.233 m<sup>2</sup> and 0.213 m<sup>2</sup> respectively. The validity of the results for each solo setup was ensured via literature comparisons with full-scale wind tunnel experiments for each respective geometry. Comparisons

were limited to experiments that used static cyclists as per the CFD simulations (no wheel rotation or pedalling), and that provided photographic or descriptive evidence that the postures adopted by the athletes were a close match to the present research (Table 1). Details on the wind tunnel experiments were extracted where possible to provide further insight into the C<sub>D</sub>A values reported in the literature. The blockage ratio (BR) is defined as the ratio of the frontal area of the cyclist to the area of the test section of a closed test section tunnel or nozzle exit area for an open test section tunnel.

Comparisons can be drawn for the upright and crouched setups, with wind tunnel experiments conducted by Kyle & Burke (1984) and Defraeye et al. (2010a), respectively. There was a 21.1% difference in C<sub>D</sub>A between the upright solo cyclist in the present study, and the full-scale experimental predictions of Defraeye et al. (2010a). However, the lower C<sub>D</sub>A predicted by Defraeye et al. (2010a) can at least partly be attributed to the use of disk wheel and a TT helmet in the experiments, which would have lowered the drag considerably in comparison to the spoked wheels and standard road helmet used in the present research. A smaller difference of 0.9% was calculated between the C<sub>D</sub>A measurements of Fintelman et al. (2014b) and the present research for the upright posture, with more closely matching bicycle and wheel geometries between both studies. A difference in C<sub>D</sub>A of 6.4% was obtained between the solo crouched postures of the present research and the wind tunnel experiment of Kyle & Burke (1984). The crouched posture adopted in the present research yielded a low C<sub>D</sub>A value only 9.4% greater than the prediction for the solo TT cyclist. However, this is due to the low torso angle and horizontal forearms. Underwood et al. (2011) and Barry et al. (2015b) both conducted studies relating aerodynamic performance to athlete posture and found trends for drag reductions with lower torso angles.

The wind tunnel experiments by Defraeye et al. (2010a) on a TT cyclist closely represented the solo TT posture adopted by the athlete used in this research. Both studies utilised static disk wheels and tear drop TT helmets. A difference in C<sub>D</sub>A of only 0.9% was found between the drag results of both studies. García-López et al. (2008) conducted wind tunnel experiments considering a TT cyclist who adopted a comparable posture to the one used in the present research. A C<sub>D</sub>A of 0.260 m<sup>2</sup> was found, 18.1% higher than the value found for the present research. However, standard spoked wheels were used by García-López et al. (2008) opposed to the disk wheels used in this research, which the larger drag predictions can be attributed to. Griffith et al. (2014) reported

a  $C_{DA}$  range between 0.20 and 0.24 m<sup>2</sup> for a range of crank positions with a TT cyclist using static wind tunnel experiments; spoked wheels were also used for this study by Griffith et al. (2014), in contrast to the disk wheels used in the present research.

In addition to the different wind tunnel operating conditions outlined in Table 1, there were further differences between the previous experimental tests (Table 1) and the present research, such as the presence of a bicycle stand in experimental studies to maintain rider and bicycle stability. The surface geometries in the present numerical study experienced some smoothing and small components were neglected for meshing purposes as per section 4.1. Anthropometric differences also existed between the athletes used in this research and the literature. However, the overall agreement between the literature and this numerical study is considered good with the correct drag trend between different postures predicted.

### 5.3. Limitations and future perspectives

Variations in torso angle may provide tangible information for athletes on how their posture influences the total drag in a tandem setup. Additional studies investigating variations in head positions, and arm positions, may yield further trends for tandem athletes for optimising the overall system. As per Barry et al. (2015b), reducing a cyclist's silhouette to improve aerodynamics though a lower frontal area might be translatable to tandem cycling; for example, for the stoker to be fully hidden behind the frontal silhouette of the pilot. Further aerodynamic improvements may be acquired through individualised posture-specific skin suits for the pilot and stoker. Existing postures adopted by athletes could potentially be adjusted to yield greater drag reductions for both the pilot and stoker, such as the FC setup providing improvements over the TT setup in this study. Fintelman et al. (2015) investigated the effect of time-trial cycling postures on physiological and aerodynamic variables, determining that trade-offs between aerodynamic drag and physiological functioning were available. The similarity of a single tandem athlete's position to that of a regular cyclist, with the added complexity of the second tandem athlete in close proximity, implies that the application of this research to tandem cycling is both relevant and may yield aerodynamic and physiological trade-offs unique to tandem cycling.

The same athlete was used for the pilot, stoker and solo athlete geometries in this study, to provide good comparison between drag predictions. However, it is recommended that individual tandem athletes with differing anthropometrics are considered for future research, to determine the influence of different anthropometric characteristics on the drag of both tandem athletes. This is emphasised by the findings from Barry et al. (2015a), who observed strong aerodynamic interactions between the drafting riders, which were attributed to be functions of individual athlete anthropometrics. Furthermore, Barry et al. (2015a) found that general trends were not consistent across tests conducted and suggested that in order to fully optimise athletes in a team, the actual athletes would be required for the analysis.

There were several limitations to this study: All the geometries considered in the CFD simulations were static, with no rotation of the wheels and no movement of the athlete's limbs. All athlete and bicycle surfaces were modelled as smooth walls, with no varying roughness of athletes' apparel and skin accounted for. All athlete surfaces were smoothed for meshing purposes. Future studies should include unique individual athletes, of different anthropometric dimensions, to provide conclusions whether particular anthropometrics are favourable for the pilot or stoker. It is noted that these findings are for numerical differences and that practical applications may differ.

## 6. Conclusions

CFD simulations were conducted to compare and provide insight into the aerodynamic performance of four tandem setups and three solo cyclist setups. Wind tunnel experiments were conducted on a single

tandem setup to provide validation data, where the largest drag deviation between CFD simulations and measurements was 4.9%. A non-biased comparison based on athlete anthropometrics was conducted for each tandem setup, by using a singular athlete for both the pilot and the stoker geometries in all tandem setups, and also for the solo rider geometries.

Two road setups and two TT setups for tandem cycling were analysed using CFD. The crouched posture combination experienced a lower aerodynamic drag than the upright posture combination as expected, with  $C_{DA}$  values of 0.314 m<sup>2</sup> and 0.413 m<sup>2</sup> measured for both setups respectively. A smaller difference in drag was recorded between the numerical results for the two TT setups, a standard TT setup and a variation termed as the frame-clench (FC) setup; where the stoker grasped the frame instead of the handlebars while the pilots retained the same position in both setups. The FC setup proved to be more favourable aerodynamically than the standard TT setup, as both the pilot and stoker experienced a lower drag than their counterparts on the standard TT setup. According to the numerical results, a  $C_{DA}$  of 0.286 m<sup>2</sup> was measured for the FC setup, 2.4% less than the TT setup, which can be translated as a gain of 8.1 s over a 10 km time-trial race. It was found that the stoker impacted the drag experienced by the pilot for this setup, providing a reduction of 9.9% for the pilot by comparison to a solo rider holding an equivalent posture, while the stoker experienced a maximum drag reduction of 58.2% in the wake of the pilot.

The benefits of providing detailed information on the aerodynamics in tandem cycling are applicable to a wide audience of athletes, coaches, manufacturers, cycling institutions and fellow researchers. By providing a non-biased baseline level of knowledge regarding tandem aerodynamics, with respect to the same identical athlete geometry being used for the pilot and the stoker, one can derive the effect of athlete anthropometrics for both respective positions. Furthermore, with greater understanding of the fundamentals of tandem aerodynamics, the potential for performance gains can be made specific to individual athletes and teams, within the rules set by the International Cycling Union (UCI).

### Conflicts of interest

None.

### Acknowledgements

The authors acknowledge the support of the College of Engineering and Informatics at the National University of Ireland, Galway. The authors acknowledge the collaboration with Paralympics Ireland, Cycling Ireland and the Sport Ireland Institute, along with the technical support team of the Department of the Built Environment at Eindhoven University of Technology: Geert-Jan Maas, Jan Diepens and Stan van Asten. The authors acknowledge the SFI/HEA Irish Centre for High-End Computing (ICHEC) for the provision of computational facilities and support, and also acknowledge the partnership with ANSYS Inc. Furthermore, the authors acknowledge and thank Corentin Cerutti from INSA Lyon for his contribution to this project in his role as a student intern. This research did not receive any specific grant from funding agencies in the public, commercial or not-for-profit sectors.

### Appendix A. Supplementary data

Supplementary data related to this article can be found at <https://doi.org/10.1016/j.jweia.2018.05.011>.

### References

- ANSYS Fluent, 2015. ANSYS Fluent Theory Guide. Release 16.1 Documentation. ANSYS Inc.
- Barry, N., Sheridan, J., Burton, D., Brown, N.A.T., 2014. The effect of spatial position on the aerodynamic interactions between cyclists. In: Proceedings of the 2014 Conference of the International Sports Engineering Association, Procedia Eng, vol.72. Elsevier B.V, pp. 774–779. <https://doi.org/10.1016/j.proeng.2014.06.131>.

- Barry, N., Burton, D., Sheridan, J., Thompson, M., Brown, N.A.T., 2015a. Aerodynamic drag interactions between cyclists in a team pursuit. *Sports Eng.* 18, 93–103. <https://doi.org/10.1007/s12283-015-0172-8>.
- Barry, N., Burton, D., Sheridan, J., Thompson, M., Brown, N.A.T., 2015b. Aerodynamic performance and riding posture in road cycling and triathlon. *Proc. Inst. Mech. Eng. P J. Sports Eng. Technol.* 229 (1), 28–38. <https://doi.org/10.1177/1754337114549876>.
- Barry, N., Burton, D., Sheridan, J., Thompson, M., Brown, N.A.T., 2016. Flow field interactions between two tandem cyclists. *Exp. Fluids* 57 (12), 1–14. <https://doi.org/10.1007/s00348-016-2273-y>.
- Blocken, B., 2014. 50 years of computational wind engineering: past, present and future. *J. Wind Eng. Ind. Aerod.* 129, 69–102. <https://doi.org/https://doi.org/10.1016/j.jweia.2014.03.008>.
- Blocken, B., 2015. Computational Fluid Dynamics for urban physics: importance, scales, possibilities, limitations and ten tips and tricks towards accurate and reliable simulations. *Build. Environ.* 91, 219–245. <https://doi.org/10.1016/j.buildenv.2015.02.015>.
- Blocken, B., Toparlar, Y., 2015. A following car influences cyclist drag: CFD simulations and wind tunnel measurements. *J. Wind Eng. Ind. Aerod.* 145 (0), 178–186. <https://doi.org/10.1016/j.jweia.2015.06.015>.
- Blocken, B., Defraeye, T., Koninckx, E., Carmeliet, J., Hespel, P., 2013. CFD simulations of the aerodynamic drag of two drafting cyclists. *Comput. Fluids* 71, 435–445. <https://doi.org/10.1016/j.compfluid.2012.11.012>.
- Blocken, B., Toparlar, Y., Andrianne, T., 2016. Aerodynamic benefit for a cyclist by a following motorcycle. *J. Wind Eng. Ind. Aerod.* 155, 1–10. <https://doi.org/https://doi.org/10.1016/j.jweia.2016.04.008>.
- Chabroux, V., Barelle, C., Favier, D., 2012. Aerodynamics of cyclist posture, bicycle and helmet characteristics in time trial stage. *J. Appl. Biomech.* 28, 317–323. [https://doi.org/10.1016/S0765-1597\(01\)00049-1](https://doi.org/10.1016/S0765-1597(01)00049-1).
- Crouch, T.N., Burton, D., LaBry, Z.A., Blair, K.B., 2017. Riding against the wind: a review of competition cycling aerodynamics. *Sports Eng.* 20 (2), 81–110. <https://doi.org/10.1007/s12283-017-0234-1>.
- Defraeye, T., Blocken, B., Koninckx, E., Hespel, P., Carmeliet, J., 2010a. Aerodynamic study of different cyclist positions: CFD analysis and full-scale wind-tunnel tests. *J. Biomech.* 43 (7), 1262–1268. <https://doi.org/10.1016/j.jbiomech.2010.01.025>.
- Defraeye, T., Blocken, B., Koninckx, E., Hespel, P., Carmeliet, J., 2010b. Computational fluid dynamics analysis of cyclist aerodynamics: performance of different turbulence-modelling and boundary-layer modelling approaches. *J. Biomech.* 43 (12), 2281–2287. <https://doi.org/10.1016/j.jbiomech.2010.04.038>.
- Artec Europe, 2017. Artec Eva, 3D scanners. Retrieved May 22, 2017, from. <https://www.artec3d.com/3d-scanner/artec-eva>.
- Fintelman, D.M., Sterling, M., Hemida, H., Li, F.-X., 2014a. Optimal cycling time trial position models: aerodynamics versus power output and metabolic energy. *J. Biomech.* 47 (8), 1894–1898. <https://doi.org/10.1016/j.jbiomech.2014.02.029>.
- Fintelman, D.M., Sterling, M., Hemida, H., Li, F.-X., 2014b. The effect of crosswinds on cyclists: an experimental study. In: The 2014 Conference of the International Sports Engineering Association, Procedia Eng, vol.72, pp. 720–725. <https://doi.org/10.1016/j.proeng.2014.06.122>.
- Fintelman, D.M., Sterling, M., Hemida, H., Li, F.-X., 2015. The effect of time trial cycling position on physiological and aerodynamic variables. *J. Sports Sci.* 414, 1–8. April 2015. <https://doi.org/10.1080/02640414.2015.1009936>.
- Franke, J., Hellsten, A., Schlünzen, H., Carissimo, B., 2007. Best practice guideline for the CFD simulation of flows in the urban environment. In: COST Action 732: Quality Assurance and Improvement of Microscale Meteorological Models. Hamburg Germany.
- García-López, J., Rodríguez-Marroyo, J.A., Juneau, C.-E., Peleteiro, J., Martínez, A.C., Villa, J.G., 2008. Reference values and improvement of aerodynamic drag in professional cyclists. *J. Sports Sci.* 26 (3), 277–286. <https://doi.org/10.1080/02640410701501697>.
- Gnehm, P., Reichenbach, S., Altpeter, E., Widmer, H., Hoppeler, H., 1997. Influence of different racing positions on metabolic cost in elite cyclists. *Med. Sci. Sports Exerc.* 29 (6), 818–823. <https://doi.org/10.1097/00005768-199706000-00013>.
- Griffith, M.D., Crouch, T., Thompson, M.C., Burton, D., Sheridan, J., 2014. Computational fluid dynamics study of the effect of leg Position on cyclist aerodynamic drag. The American Society of Mechanical Engineers. *J. Fluid Eng.* 136. <https://doi.org/10.1115/1.4027428>.
- Kyle, C.R., Burke, E.R., 1984. Improving the racing bicycle. *Mech. Eng.* 106 (9), 34–45.
- Lukes, R. a, Chin, S.B., Haake, S.J., 2005. The understanding and development of cycling aerodynamics. *Sports Eng.* 8, 59–74. <https://doi.org/10.1007/BF02844004>.
- Mannion, P., Toparlar, Y., Blocken, B., Hajdukiewicz, M., Andrianne, T., Clifford, E., 2017. Improving CFD prediction of drag on Paralympic tandem athletes: influence of grid resolution and turbulence model. *Sports Eng.* 21 (2), 123–135. <https://doi.org/10.1007/s12283-017-0258-6>.
- Menter, F.R., 1994. Two-equation eddy-viscosity turbulence models for engineering applications. *AIAA J.* 32 (8), 1598–1605. <https://doi.org/10.2514/3.12149>.
- Mercker, E., Wiedemann, J., 1996. On the correction of interference effects in open jet wind tunnels. *SAE International*, 960671. ISSN 0148-7191. <https://doi.org/10.4271/960671>.
- Oggiano, L., Leirdal, S., Saetran, L., Ettema, G., 2008. Aerodynamic optimization and energy saving of cycling postures for international elite level cyclists. *Eng. Sport* 1 (2), 597–604, 7. [https://doi.org/10.1007/978-2-287-09411-8\\_70](https://doi.org/10.1007/978-2-287-09411-8_70).
- Tominaga, Y., Mochida, A., Yoshie, R., Kataoka, H., Nozu, T., Yoshikawa, M., Shirasawa, T., 2008. AIJ guidelines for practical applications of CFD to pedestrian wind environment around buildings. *J. Wind Eng. Ind. Aerod.* 96 (10–11), 1749–1761. <https://doi.org/10.1016/j.jweia.2008.02.058>.
- UCI, 2017. Cycling Regulations, Part 16 Para-cycling, Version on 01/02/2017. Union Cycliste Internationale. Retrieved from. [http://www.uci.ch/mm/Document/News/Rulesandregulation/16/26/73/16-PAR-20170201-E\\_English.PDF](http://www.uci.ch/mm/Document/News/Rulesandregulation/16/26/73/16-PAR-20170201-E_English.PDF).
- Underwood, L., Jermy, M., 2010. Optimal hand position for individual pursuit athletes. *Procedia Eng.* 2 (2), 2425–2429. <https://doi.org/10.1016/j.proeng.2010.04.010>.
- Underwood, L., Schumacher, J., Burette-Pommay, J., Jermy, M., 2011. Aerodynamic drag and biomechanical power of a track cyclist as a function of shoulder and torso angles. *Sports Eng.* 14 (2–4), 147–154. <https://doi.org/10.1007/s12283-011-0078-z>.